THE JOURNAL OF BIOLOGICAL CHEMISTRY VOL. 290, NO. 23, pp. 14595–14609, June 5, 2015

L-Serine Deficiency Elicits Intracellular Accumulation of Cytotoxic Deoxysphingolipids and Lipid Body Formation*

Received for publication, August 8, 2014, and in revised form, April 11, 2015 Published, JBC Papers in Press, April 22, 2015, DOI 10.1074/jbc.M114.603860

Kayoko Esaki[‡§¶1], Tomoko Sayano[‡¶], Chiaki Sonoda[‡], Takumi Akagi[‖], Takeshi Suzuki[**], Takuya Ogawa[‡‡], Masahiro Okamoto[§§], Takeo Yoshikawa[§], Yoshio Hirabayashi[¶], and Shigeki Furuya[‡§§2]**

From the [‡]Laboratories of Functional Genomics and Metabolism and [**]Synthetic Biology, Division of Systems Bioengineering, Graduate School of Bioresource and Bioenvironmental Sciences, and [§§]Bio-Architecture Center, Kyushu University, Fukuoka 812-8581, the Laboratories for [§]Molecular Psychiatry and [¶]Molecular Membrane Neuroscience, [‖]Support Unit for Neuromorphological Analysis, RIKEN Brain Science Institute, Wako-shi, Saitama 351-0198, and the [‡‡]Department of Pharmaceutical Sciences, International University of Health and Welfare, Tochigi 324-8501, Japan

Background: L-Serine deficiency affects sphingolipid homeostasis.
Results: Reduced L-serine promotes the accumulation of 1-deoxysphingolipids and the formation of lipid bodies.
Conclusion: Diminished capacity for L-serine synthesis leads to a higher L-alanine to L-serine ratio and elicits the synthesis of 1-deoxysphingolipids and lipid body formation.
Significance: 1-Deoxysphingolipids occur in certain disease conditions characterized by a metabolic imbalance between L-alanine and L-serine.

L-Serine is required to synthesize membrane lipids such as phosphatidylserine and sphingolipids. Nevertheless, it remains largely unknown how a diminished capacity to synthesize L-serine affects lipid homeostasis in cells and tissues. Here, we show that deprivation of external L-serine leads to the generation of 1-deoxysphingolipids (doxSLs), including 1-deoxysphinganine, in mouse embryonic fibroblasts (KO-MEFs) lacking D-3-phosphoglycerate dehydrogenase (Phgdh), which catalyzes the first step in the *de novo* synthesis of L-serine. A novel mass spectrometry-based lipidomic approach demonstrated that 1-deoxydihydroceramide was the most abundant species of doxSLs accumulated in L-serine-deprived KO-MEFs. Among normal sphingolipid species in KO-MEFs, levels of sphinganine, dihydroceramide, ceramide, and hexosylceramide were significantly reduced after deprivation of external L-serine, whereas those of sphingomyelin, sphingosine, and sphingosine 1-phosphate were retained. The synthesis of doxSLs was suppressed by supplementing the culture medium with L-serine but was potentiated by increasing the ratio of L-alanine to L-serine in the medium. Unlike with L-serine, depriving cells of external L-leucine did not promote the occurrence of doxSLs. Consistent with results obtained from KO-MEFs, brain-specific deletion of *Phgdh* in mice also resulted in accumulation of doxSLs in the brain. Furthermore, L-serine-deprived KO-MEFs exhibited increased formation of cytosolic lipid bodies containing doxSLs and other sphingolipids. These *in vitro* and *in vivo* studies indicate that doxSLs are generated in the presence of a high ratio of L-alanine to L-serine in cells and tissues lacking *Phgdh*, and *de novo* synthesis of L-serine is necessary to maintain normal sphingolipid homeostasis when the external supply of this amino acid is limited.

L-Serine, a nonessential (dispensable) amino acid, is synthesized *de novo* from a glycolytic intermediate, 3-phosphoglycerate, through three catalytic steps known as the phosphorylated pathway (1). The first step in this pathway is catalyzed by D-3-phosphoglycerate dehydrogenase (PHGDH,[3] EC1.1.1.95) (2). Humans with mutated *PHGDH* have lower levels of free L-Ser in the plasma and in cerebrospinal fluid. These L-Ser-deficient patients exhibit severe neurological symptoms, including congenital microcephaly, psychomotor retardation, and intractable seizures (3–5). In addition to these data from humans with *PHGDH* deficiency, our *in vivo* study demonstrated that conventional *Phgdh* knock-out (KO) mice display severe consequences of embryonic development, such as brain malformation with overall growth retardation, and die after embryonic day 13.5 (6–8). These human and mouse studies highlighted the absolute necessity of L-Ser, synthesized *de novo* via the phosphorylated pathway, for embryonic viability and nervous system development. In addition, recent functional genomic studies showed that *de novo* biosynthesis of L-Ser plays a crucial role in invasiveness, malignant transformation, and proliferation of certain types of cancer (9, 10). L-Ser also acts on pyruvate kinase M2 as an allosteric effector and supports aerobic glycolysis, which is a metabolic hallmark of cancer cells (9, 10). These reports provide unexpected evidence that enhanced L-Ser availability in the body is involved in intrinsic metabolic reprogramming of cancer cells.

* This work was supported in part by a grant from The Tojuro Iijima Foundation for Food and Technology (to S. F.) and Japan Society for the Promotion of Science KAKENHI Grant 14J05809 (to K. E.).
[1] Supported by the fellowship of Junior Research Associate of RIKEN.
[2] To whom correspondence should be addressed: Division of Systems Bioengineering, Graduate School of Bioresource and Bioenvironmental Sciences, Kyushu University, Fukuoka 812-8581, Japan. Tel./Fax: 81-92-642-7604; E-mail: shigekifur@brs.kyushu-u.ac.jp.

[3] The abbreviations used are: PHGDH, D-3-phosphoglycerate dehydrogenase; BKO, brain-specific *Phgdh* knock-out; SL, sphingolipid; MEF, mouse embryonic fibroblast; SPT, serine palmitoyltransferase; HSAN1, hereditary sensory and autonomic neuropathy type I; doxSL, 1-deoxysphingolipid; SA, sphinganine; SO, sphingosine; Cer, ceramide; DHCer, dihydroceramide; HexCer, hexosylceramide; LacCer, lactosylceramide; SM, sphingomyelin; ER, endoplasmic reticulum; EMEM, Eagle's minimum essential medium.

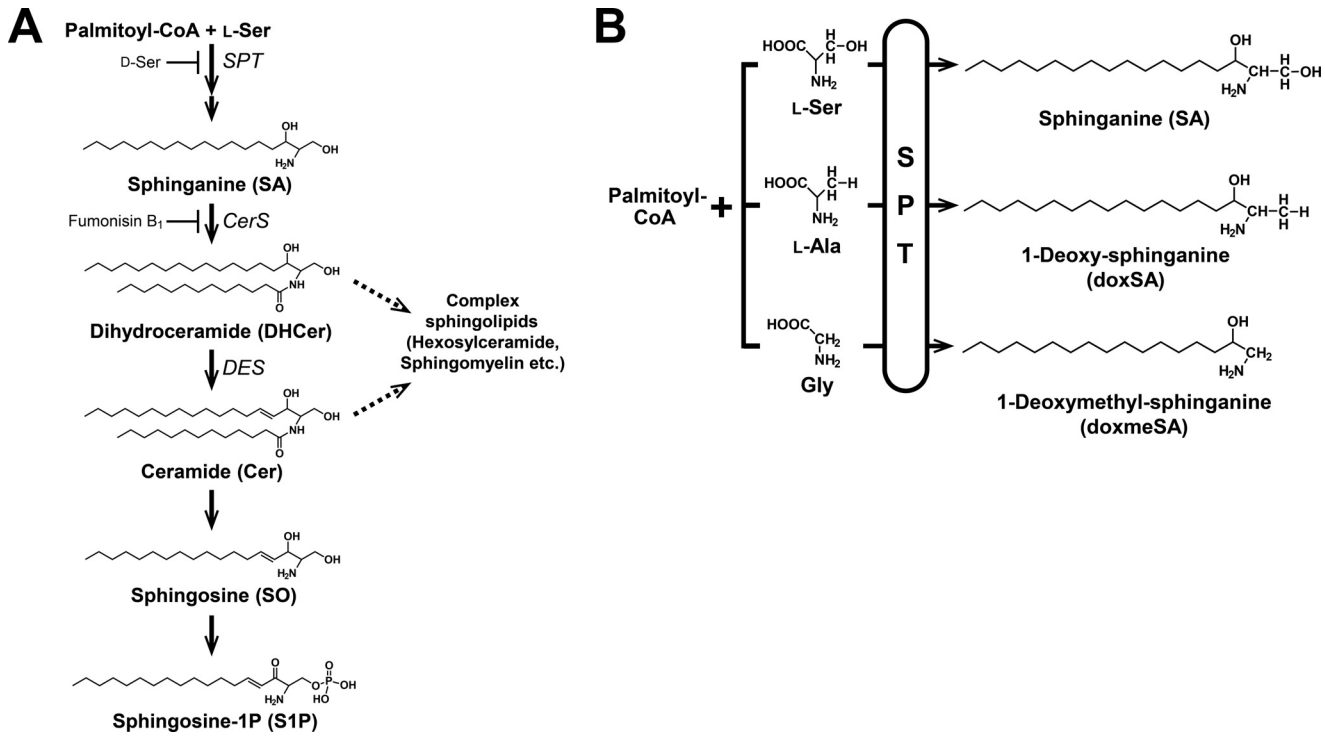

FIGURE 1. **Sphingolipid biosynthetic pathway.** *A,* L-Ser and palmitoyl-CoA are condensed by SPT to form 3-keto-sphinganine, which is reduced to SA. Then, SA is *N*-acylated to form DHCer and desaturated to form Cer. In addition, Cer is converted to SO and subsequently phosphorylated to generate sphingosine 1-phosphate (*S1P*) by the degradative pathway. *B,* sphingoid bases generated by SPT, which uses not only L-Ser but also L-Ala or Gly as a substrate and synthesizes atypical doxSLs. Because of the lack of the C1 hydroxyl group, doxSLs can neither be converted to complex sphingolipids nor degraded by the degradative pathway.

We recently demonstrated that brain-specific *Phgdh* knockout (BKO) mice exhibit marked reductions in both L- and D-Ser levels in the brain, accompanied by diminished *N*-methyl-D-aspartate (NMDA) receptor function (11). These results indicate that L-Ser synthesized *de novo* in the brain determines the availability of D-Ser and indirectly regulates higher functions via NMDA receptor-mediated transmission. Nonetheless, it remains unclear how the diminished L-Ser synthesis elicits alterations in L-Ser-derived metabolites other than D-Ser.

Unlike other amino acids, L-Ser is used directly for the synthesis of phosphatidylserine and ceramide, the hydrophobic moiety of sphingolipids (SLs). The latter SLs act as important mediators of the signaling cascades involved in various cellular functions, such as apoptosis, proliferation, and the stress response (12). The first step of SL synthesis is the condensation of L-Ser and palmitoyl-CoA catalyzed by serine palmitoyltransferase (SPT), which is a rate-limiting enzyme in the SL synthetic pathway (Fig. 1*A*) (13, 14). Our previous analysis of membrane lipids in embryonic tissues of conventional *Phgdh* KO mice showed that L-Ser deficiency resulting from *Phgdh* deletion leads to drastic reduction of major SLs such as GD3 (7), prompting us to investigate the consequences of L-Ser deficiency on SL homeostasis in cells and tissues.

In this study, to determine the effect of L-Ser deficiency on SL metabolism at the molecular level, we developed a novel mass spectrometry-based lipidomic system and examined whether diminished synthesis of L-Ser caused by genetic ablation of *Phgdh* altered the metabolism of SLs in KO-mouse embryonic fibroblasts (MEFs) and BKO mice. Here, we report that reduced availability of L-Ser led to a decrease in normal SLs and elicited the synthesis and accumulation of 1-deoxysphinganine (doxSA) and its derivatives (Fig. 1*B*).

Experimental Procedures

Materials—The internal standard mixture (ceramide/sphingoid internal standard mixture II), 1-deoxysphinganine (doxSA, m18:0), 1-deoxysphingosine (doxSO, m18:1), 1-deoxymethylsphinganine (doxmeSA, m17:0), 1-deoxymethylsphingosine (doxmeSO, m17:1), *N*-lauroyl (C12)-DHCer, C12–1-deoxydihydroceramide (C12doxDHCer), and C12–1-deoxyceramide (C12doxCer) were purchased from Avanti Polar Lipids (Alabaster, AL).

Cell Culture—Spontaneously immortalized MEFs were established from individual E13.5 embryos of wild-type (WT) and *Phgdh* KO mice (15). KO-MEFs transduced retrovirally with the mouse *Phgdh* cDNA (KO-MEF^{+Phgdh}) were generated as described below. Retroviral gene transfer was performed according to published procedures (16). Briefly, mouse *Phgdh* cDNA obtained by RT-PCR using cDNA prepared from mouse bone marrow macrophages was cloned into the pTAC-1 vector (BioDynamics Laboratory). DNA fragment containing N-terminal HA-tagged *Phgdh* cDNA was subcloned into the retroviral expression vector pCX4bsr (GenBank^{TM} accession number AB086384, a gift from Dr. Tsuyoshi Akagi, *KAN* Research Institute, Kobe, Japan). To prepare the retrovirus, the expression vector plasmid for *Phgdh* (pCX4-HA-mPhgdh-ires-bsr) was introduced into the packaging cell line Platinum-E (17) with the vectors pE-eco and pGP (Takara) by using polyethyleneimine

"Max" (Polysciences), and the transfected cells were cultured for 48 h. The supernatant was collected, filtered through a 0.45-μm filter, and used as the retrovirus stock. For infection, KO-MEFs were incubated with the viral stock diluted 1:1 in fresh medium containing a final concentration of 4 μg/ml Polybrene (Sigma) and incubated overnight at 33 °C. The infection was repeated at 6 and 18 h after the initial infection. 24 h after the last infection, the cells were washed four times with PBS, and then infected cells were selected in medium containing 10 μg/ml blasticidin S (Kaken Pharmaceutical) at 37 °C for 2 to 3 days until 100% of the uninfected MEFs were killed. The drug-resistant KO-MEFs were used for assay. All cell lines were cultured in Dulbecco's modified Eagle's medium (DMEM, high glucose; Wako Pure Chemical Industries Ltd., Osaka, Japan) with 10% fetal bovine serum (FBS; ICN Biomedicals, Inc., Aurora, OH) and 10 μg/ml gentamicin (Nacalai Tesque, Kyoto, Japan). To treat MEFs under L-Ser-supplemented or -deprived conditions, the culture medium was replaced with Eagle's minimum essential medium with Earle's salts (EMEM; Wako Pure Chemical Industries Ltd.) containing 1% FBS and gentamicin, with or without 400 μM L-Ser. EMEM does not contain glycine, L-Ala, or L-Ser. We previously observed that this L-Ser-deprived condition significantly induced *Eif4ebp1* mRNA encoding eukaryotic initiation factor 4-binding protein 1 after 6 h in KO-MEFs (15). Enhanced phosphorylation of eIF2α (α subunit of eukaryotic translation initiation factor 2) and increased mRNA expression of *Gadd34/Ppp1r15a* (encoding protein phosphatase 1, regulatory subunit 15A) and *Chop/Ddit3* (encoding CCAAT/enhancer binding protein homologous protein/DNA-damage inducible transcript 3) also occurred when KO-MEFs were cultured under this L-Ser-deprived condition. These changes are indicative of the activation of amino acid starvation responses mediated by GCN2-eIF2α-ATF4, suggesting that the employed L-Ser-deprived condition resulted in cellular L-Ser deficiency in KO-MEFs. When examining the effect of L-leucine deprivation, the medium was replaced with DMEM (deficient in L-leucine, L-arginine, and L-lysine, low glucose; Sigma-Aldrich Japan; Tokyo, Japan) containing 1% FBS, gentamicin, 800 μM L-Lys, and 400 μM L-Arg, with or without 800 μM L-Leu.

The effects of doxSA on growth of KO-MEFs, WT-MEFs, and HeLa cells were examined by culturing the cells in EMEM containing 400 μM L-Ser with either SA (5 μM) or doxSA (0.01, 0.1, 1, or 5 μM). After incubation for 24 or 48 h, cell viability was examined using the trypan blue exclusion method. HeLa cells were kindly provided by Prof. Sanetaka Shirahata of Kyushu University.

Animals—Floxed mice (*Phgdh*$^{flox/flox}$) and BKO mice (*hGFAP*$^{+/Cre}$: *Phgdh*$^{flox/flox}$) were maintained in a 12-h light/dark cycle with unlimited access to water and laboratory chow containing 20% casein. The brains were excised from 10–12-week-old female mice (floxed, $n = 7$; BKO, $n = 8$) as quickly as possible. The hippocampus was isolated on an ice-cooled glass plate, flash-frozen in liquid N_2, freeze-dried, and stored at −20 °C until sphingolipid analysis. Protocols for the animal experiments were approved by the Animal Ethics Committees of Kyushu University.

Amino Acid Analysis—The amino acid analysis in MEFs was performed as described previously (15). Briefly, MEFs were homogenized in 100 μl of distilled water, and proteins in the homogenate were removed by adding 10 μl of 5% perchloric acid. The supernatants were centrifuged at 15,000 rpm for 20 min at 4 °C and adjusted to neutral pH by adding 8 M KOH. Then, they were centrifuged at 15,000 rpm for 10 min at 4 °C. The amino acid content of the supernatants was determined on an amino acid analyzer (L-8500; Hitachi).

Isolation of Lipid Body Fraction—Lipid body isolation from KO-MEFs was carried out according to published procedures with modifications (18). In brief, KO-MEFs were washed twice with Dulbecco's phosphate-buffered saline (DPBS) and scraped from the dish. The pellet of ~3–5 × 10^7 cells was resuspended in 400 μl of cold DPBS, sonicated, and centrifuged at 13,500 rpm for 5 min at 4 °C. The supernatant was mixed with an equal volume of 2 M sucrose in 20 mM Tris-HCl, pH 7.5. The mixture was placed at the bottom of the ultracentrifuge tube (343778, Beckman) and overlaid with 0.2 M sucrose in 20 mM Tris-HCl, pH 7.5 (0.15× volume of the mixture). The tube was ultracentrifuged at 55,000 rpm (Optima XL-100 K, Beckman) for 2.5 h at 4 °C. After the centrifugation, the white top layer fraction containing lipid bodies (100 μl) was collected. The collected fraction was used for lipid analysis as described below.

Lipid Extraction—SLs were extracted using the method of Shaner *et al.* (19). Cells were washed twice with DPBS and scraped from the dish. The pellet of ~2–10 × 10^6 cells was resuspended in 400 μl of cold DPBS and sonicated. After addition of 1.5 ml of chloroform/methanol (1:2, v/v), 25 pmol of internal standard was added to the homogenate. The solution was sonicated for 30 s and incubated at 48 °C overnight. After addition of 150 μl of 1 M KOH in methanol, the mixture was sonicated for several seconds, incubated for 2 h at 37 °C, and neutralized by adding glacial acetic acid. For sphingoid base analysis, the samples were centrifuged at 2500 rpm for 10 min to obtain the supernatant. The residue was re-extracted with 1 ml of chloroform/methanol (2:1, v/v) and centrifuged at 2500 rpm for 10 min. The supernatants were combined. For ceramide analysis, after 1 ml of chloroform and 2 ml of water had been added, the samples were vortexed well and centrifuged at 2500 rpm for 10 min to obtain a two-phase system, the aqueous top and the organic bottom phase, from which lipids were extracted. The top phase was re-extracted with an additional 1 ml of chloroform. The solution was vortexed well and centrifuged at 2500 rpm for 10 min, and the organic phases were combined. These lipid extracts were dried under an N_2 stream and stored at −20 °C until use. The dried residue was dissolved in the mobile phase solvent immediately before liquid chromatography electrospray ionization tandem mass spectrometry (LC/ESI-MS/MS) analysis.

Liquid Chromatography and Mass Spectrometry—High performance liquid chromatography (HPLC) was performed on an Agilent 1100 series instrument (Agilent Technologies, Santa Clara, CA). A Capcell Pak C18 MGIII column (50 × 2.0 mm inner diameter, 3 μm, Shiseido Co., Ltd., Tokyo, Japan) was used for sphingoid base analysis, and a Cosmosil-packed col-

TABLE 1
Mass spectrometer settings for sphingoid bases

Sphingoid base	Q1 *m/z*	Q3 *m/z*
d17:0 SA	288	60
d18:0 SA	302	60
d17:1 SO	286	250
d18:1 SO	300	264
d17:1 S1P	366	264
d18:1 S1P	380	264
m17:0 doxmeSA	272	254
m18:0 doxSA	286	268
m17:1 doxmeSO	270	252
m18:1 doxSO	284	266

TABLE 2
Mass spectrometer settings for ceramides and their metabolites

	N-Acyl	Q1 *m/z*	Q3 *m/z*
DHCer	C12:0	484	266
	C16:0	540	266
	C18:0	568	266
	C20:0	596	266
	C22:0	624	266
	C24:0	652	266
	C24:1	650	266
doxDHCer	C12:0	468	268
	C16:0	524	268
	C18:0	552	268
	C20:0	580	268
	C22:0	608	268
	C24:0	636	268
	C24:1	634	268
Cer	C12:0	482	264
	C16:0	538	264
	C18:0	566	264
	C20:0	594	264
	C22:0	622	264
	C24:0	650	264
	C24:1	648	264
doxCer	C12:0	466	266
	C16:0	522	266
	C18:0	550	266
	C20:0	578	266
	C22:0	606	266
	C24:0	634	266
	C24:1	632	266
LacCer	C12:0	806	264
	C16:0	862	264
	C18:0	890	264
	C20:0	918	264
	C22:0	946	264
	C24:0	974	264
	C24:1	972	264
HexCer	C12:0	644	264
	C16:0	700	264
	C18:0	728	264
	C20:0	756	264
	C22:0	784	264
	C24:0	812	264
	C24:1	810	264
SM	C12:0	647	184
	C16:0	703	184
	C18:0	731	184
	C20:0	759	184
	C22:0	787	184
	C24:0	815	184
	C24:1	813	184

umn $5C_8$-MS (150 × 2.0 mm inner diameter, 5 μm, Nacalai Tesque) for ceramide analysis. The HPLC mobile phases for sphingoid base analysis were as follows: A1, methanol/water (60:40, v/v) containing 0.1% formic acid and 5 mM ammonium formate; B1, methanol containing 0.1% formic acid and 5 mM ammonium formate. The HPLC mobile phases for ceramide analysis were as follows: A2, water containing 0.2% formic acid and 5 mM ammonium formate; B2, methanol containing 0.2% formic acid and 5 mM ammonium formate. A gradient program was used for the HPLC separation at a flow rate of 0.2 ml/min. The gradient elution program for sphingoid base analysis consisted of holding at 40% B1 for 6 min, linearly increasing to 100% B1 over 10 min, and maintaining it for 5 min, followed by re-equilibration to the initial condition for 16–20 min. In the case of ceramide analysis, the initial mobile phase was 80% B2, then was linearly changed to 90% B2 over 3 min, followed by a second linear gradient to 95% B2 over 3 min, and then a third linear gradient to 99% B2 over 15 min. The chromatography was terminated with isocratic elution at 99% B2 for 8.5 min. The column was equilibrated with 80% B2 for 30–33 min.

The HPLC system was coupled to a 4000 QTRAP hybrid triple quadrupole/linear ion trap mass spectrometer (AB SCIEX; Framingham, MA) equipped with a Turbo Ion Spray source. The mass spectrometer was run in the positive mode with the curtain gas set at 10 and interface heater "on." Ion spray voltage was used with optimal values for analysis of a sphingoid base as follows: DHCer and doxDHCer; Cer and doxCer; lactosylceramide (LacCer), hexosylceramide (HexCer); and sphingomyelin (SM) set at 5500, 4000, 5000, and 4000. Similarly, parameters of the temperature, nebulizer gas, and auxiliary gas were set at 550, 25, and 45 for a sphingoid base; 475, 20, and 70 for DHCer and doxDHCer; 325, 32.5, and 60 for Cer and doxCer; and 375, 40, and 50 for lactosylceramide, hexosylceramide, and sphingomyelin, respectively. Identification of structure-specific fragments was performed in product ion scan mode. Multiple reaction monitoring of ions of each sphingolipid is shown in Tables 1 and 2. Data acquisition and analysis were performed using Analyst Software version 1.4.1 (AB SCIEX). The quantified lipids were normalized to the cell number and the internal standard.

Fluorescence Microscopy and Electron Microscopy—For fluorescence microscope observation, KO-MEFs were grown on a glass-bottom dish for 48 h and stained with 1:2000-fold medium volume of Nile Red solution (Sigma; 1 mg/ml in ethanol) for 1 h. KO-MEFs were observed under an Olympus FV1000 confocal microscope. For electron microscopic observation, KO-MEFs, grown on a low fluorescence plastic film (LF1, Sumitomo Bakelite; MS-92132) for 24 h, were washed with DPBS and fixed with freshly made fixing solution (2% paraformaldehyde and 2.5% glutaraldehyde in 0.1 M phosphate buffer, pH 7.2) for 2 h at room temperature. After fixation, KO-MEFs were washed with DPBS and processed for electron microscopic observation. KO-MEFs were post-fixed with 1% osmium tetraoxide, dehydrated through a gradient series of ethanol, and then embedded in EPON 812 epoxy resin. The thin sections (80 nm) were cut and stained with uranium acetate and lead citrate and examined under a Tecnai 12 electron microscope (FEI, Hillsboro, OR).

Statistics—The data are presented as mean ± S.E. from at least three independent experiments. Differences between two groups were examined using the Student's *t* test. Differences among more than two groups were analyzed using one-way analysis of variance with the subsequent Tukey-Kramer test. The statistical significance of differences was set at $p < 0.05$. All calculations were performed using KaleidaGraph 4.0 software (Synergy Software, Reading, PA).

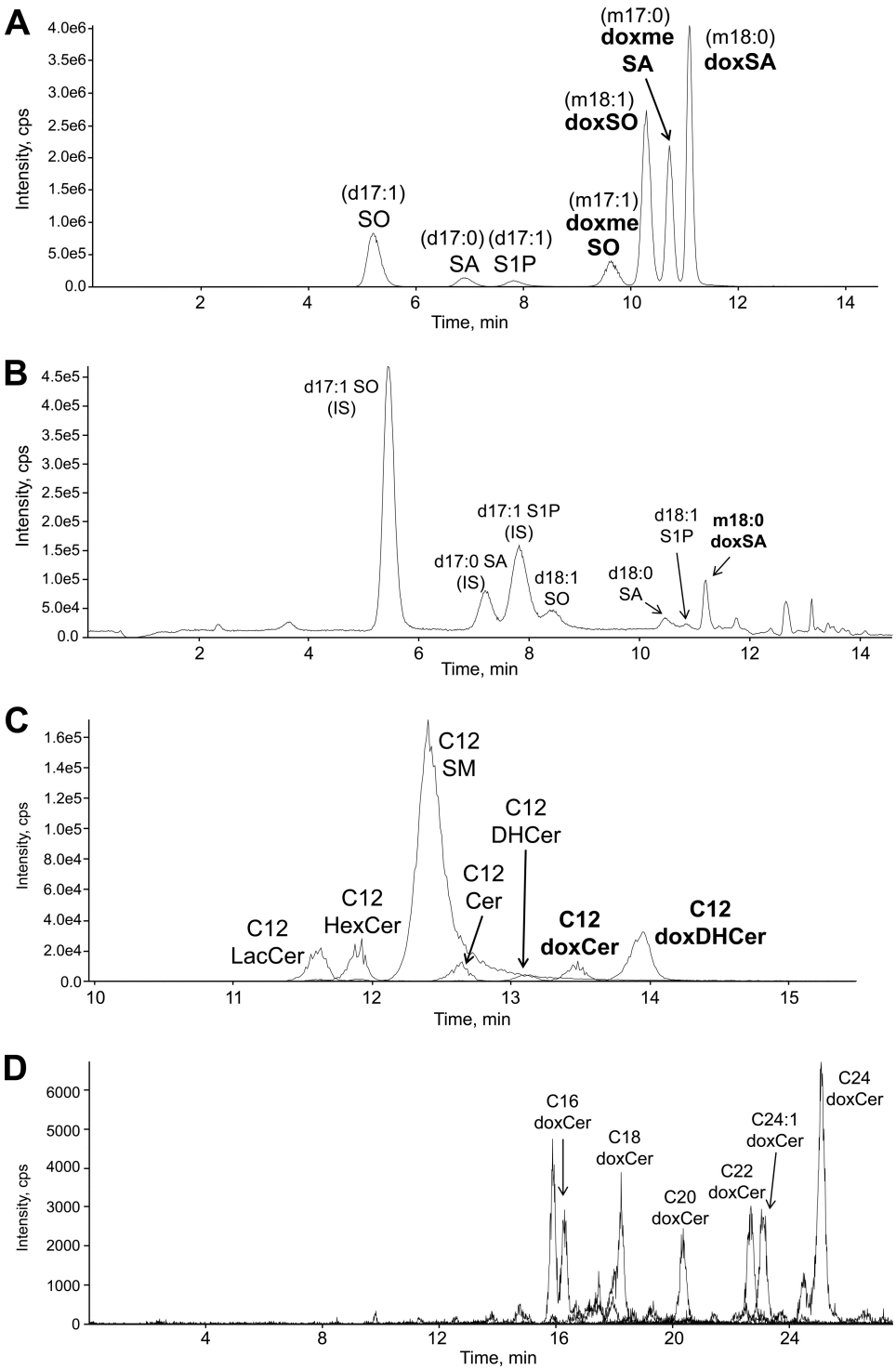

FIGURE 2. **Selected LC-MS/MS ion chromatograms of free sphingoid bases, ceramides, and their metabolites.** *A* and *C,* standard mixtures; *B* and *D,* extracts of *Phgdh* KO-MEFs. *D* shows an ion chromatogram of doxCer from the lipid extract of KO-MEFs. Abbreviations used are as follows: *IS,* internal standard; *S1P*, sphingosine 1-phosphate.

Results

Establishment of Methods for Quantitative Analysis of Sphingolipids—We recently demonstrated that external L-Ser deprivation results in a significant 70% reduction of intracellular free L-Ser in KO-MEFs after 6 h (15). To monitor the detailed composition of SLs in L-Ser-deprived KO-MEFs, we established methods for quantitative analysis of sphingolipids using LC/ESI-MS/MS. Free sphingoid bases were analyzed using reversed-phase HPLC on a C18 column according to published procedures (19–21). Because doxSA and sphingosine (SO) have almost the same mass, they were distinguished by the difference in retention time (Fig. 2*A*). For the analysis of *N*-acyl-derivatives of sphingoid bases, including ceramide, we developed a novel analytical method by means of reversed-phase

HPLC on a C8 column, which is applicable for most *N*-acyl-derivatives (Fig. 2*C*).

As shown in Fig. 2, *B* and *D*, lipid extracts of KO-MEFs were analyzed using the above-mentioned optimized HPLC conditions; major sphingolipids, including sphingoid bases, Cer, and their metabolites, were successfully identified. This novel LC/ESI-MS/MS analysis does not require the chemical hydrolysis of sphingolipids and thereby allows us to distinguish molecular forms of *N*-acyl-derivatives of normal sphingoid and 1-deoxysphingoid bases.

L-Serine Deficiency Promoted Biosynthesis of doxSLs—We analyzed SLs of KO-MEFs maintained in the presence or absence of L-Ser for 6 and 24 h. The L-Ser-deprived medium contains 4 μM L-Ser, which is derived from the 1% FBS, and the L-Ser-supplemented medium contains 400 μM L-Ser from the added L-Ser solution. Compared with the composition of SLs under the L-Ser-supplemented condition, KO-MEFs maintained for 6 h under the L-Ser-deprived condition exhibited significantly lower levels of normal SA, DHCer, and Cer. Meanwhile, the occurrence of doxSLs, such as doxSA, doxmeSA, doxDHCer, and doxCer, was detected in KO-MEFs under the L-Ser-deprived condition (Fig. 3). Although the levels of HexCer in KO-MEFs decreased significantly after L-Ser deprivation for 24 h, the amounts of SO, sphingosine 1-phosphate, LacCer, and SM did not differ between the two conditions (Fig. 3). Incubation with L-Ser-deprived culture medium for 6 and 24 h elicited a 7.1- and a 30.6-fold increase in doxSA, respectively, in KO-MEFs compared with those under the L-Ser-supplemented condition (Fig. 3). We detected a higher level of doxSA than doxmeSA. This is because glycine, a precursor of doxmeSA, is reduced significantly in MEFs under L-Ser-deprived conditions (15). In addition to doxSA, we found that doxDHCer was the most abundant species of doxSLs that accumulated in KO-MEFs (Fig. 3). It is noteworthy in L-Ser-deprived KO-MEFs that long chain fatty acids such as C22:0, C24:0, and C24:1 dominated in the fatty acid compositions of doxDHCer and doxCer compared with normal SLs (Fig. 4). Next, we found that doxSA occurred in KO-MEFs^{+Phgdh} and WT-MEFs under the L-Ser-deprived condition, although their amounts were much lower than those observed in L-Ser-deprived KO-MEFs (Fig. 5, *A* and *B*), indicating that reduced L-Ser availability led to the generation of doxSLs at a low level even in cells able to synthesize L-Ser *de novo*. In contrast, L-Leu deprivation did not promote the synthesis of doxSLs (Fig. 5*C*). Thus, doxSLs in the cells serve as sensitive biomarkers for reduced availability of intracellular L-Ser.

doxSL Accumulation in the Brain of BKO Mice—BKO mice carrying a brain-specific deletion of *Phgdh* exhibit a dramatic reduction in both L- and D-Ser levels in the brain, and this is associated with mild microcephaly and atrophy of the forebrain, including the cerebral cortex and hippocampus (11). To confirm that the occurrence of doxSLs is a result of L-Ser deficiency *in vivo*, we analyzed SLs in the hippocampus of BKO mice. The LC/ESI-MS/MS analysis demonstrated that the amount of doxSA in the BKO hippocampus was ~3.5-fold higher than that in the control floxed hippocampus. Similarly, the BKO hippocampus displayed a significantly elevated level of doxDHCer (Fig. 6), whereas no significant changes in total Cer and DHCer contents were found between the BKO hippocampus and the floxed brain (Figs. 6 and 7). Furthermore, the amounts of complex SLs (HexCer, LacCer, and SM) were also not significantly reduced in the BKO brain (Fig. 6). Unlike the major Cer and DHCer species present in KO-MEFs, the fatty acid C16:0 was not detected, and C18:0 was the major chain length of doxCer in the brain of BKO mice. In addition, the fatty acid composition of doxDHCer differed from that of other SLs in the BKO brain (Fig. 7). These observations showed that the *in vivo* L-Ser deficiency in the brain also led to accumulation of doxSLs, as seen in KO-MEFs. These results raise the possibility that doxSLs may be involved in the pathogenesis of central neurological symptoms seen in human patients with genetic L-Ser deficiency disorders.

Suppression of doxSLs Synthesis by D-Ser—To test whether SPT catalyzes the condensation of L-Ala with palmitoyl-CoA under the L-Ser-deprived condition, we examined the effects of D-Ser treatment of KO-MEFs on the generation of doxSLs. D-Ser is naturally generated from L-Ser by serine racemase in the mammalian nervous system (22), whereas SPT activity is inhibited by D-Ser through substrate competition with L-Ser for the amino acid recognition site (23). As shown in Fig. 8*A*, the addition of D-Ser to the culture medium significantly suppressed the generation of doxSA as well as normal SLs, confirming that doxSLs are synthesized by the reaction of SPT.

Higher Ratio of L-Ala to L-Ser Promoted doxSL Biosynthesis in KO-MEFs—The above findings raise the possibility that a higher ratio of L-Ala to L-Ser within cells promotes biosynthesis of doxSLs by SPT. To test this possibility, we used the LC/ESI-MS/MS system to examine the effect of a higher ratio L-Ala to L-Ser in the culture medium on the production of doxSLs in KO-MEFs. When KO-MEFs were deprived of L-Ser but supplemented with 400 μM L-Ala, the doxSLs levels increased more prominently than under other conditions examined (Fig. 8*B*). Incubation of KO-MEFs in a culture medium with a 4:1 ratio of L-Ala to L-Ser also resulted in doxSLs reaching levels seen in L-Ser-deprived KO-MEFs (Fig. 8*C*). In contrast, a 1:1 ratio of L-Ala to L-Ser suppressed the production of doxSLs (Fig. 8*B*). Under the L-Ser-deprived condition, the intracellular molar ratio of L-Ala/L-Ser in KO-MEFs was estimated to be >3.0, which was much higher than that in KO-MEFs maintained under the L-Ser-supplemented condition or in WT-MEFs (Table 3). Thus, the increased ratio of L-Ala to L-Ser is a likely cause of production of doxSLs in MEFs with reduced L-Ser availability.

doxSA Inhibited Cell Proliferation—Exogenous addition of doxSA reduced the proliferation of cancer cells (24) and caused cell death in various cell lines (24, 25). Therefore, to test whether doxSA also exerts a cytotoxic effect on nonmalignant KO-MEFs and WT-MEFs in the presence of L-Ser, we compared their proliferation with HeLa cells. KO-MEFs can proliferate in the presence of L-Ser, but their proliferation is suppressed when deprived of L-Ser.[4] Unlike KO-MEFs, the proliferation of WT-MEFs and HeLa cells was not affected by the absence of L-Ser in the culture medium (data not shown).

[4] T. Sayano, Y. Hirabayashi, and S. Furuya, unpublished observations.

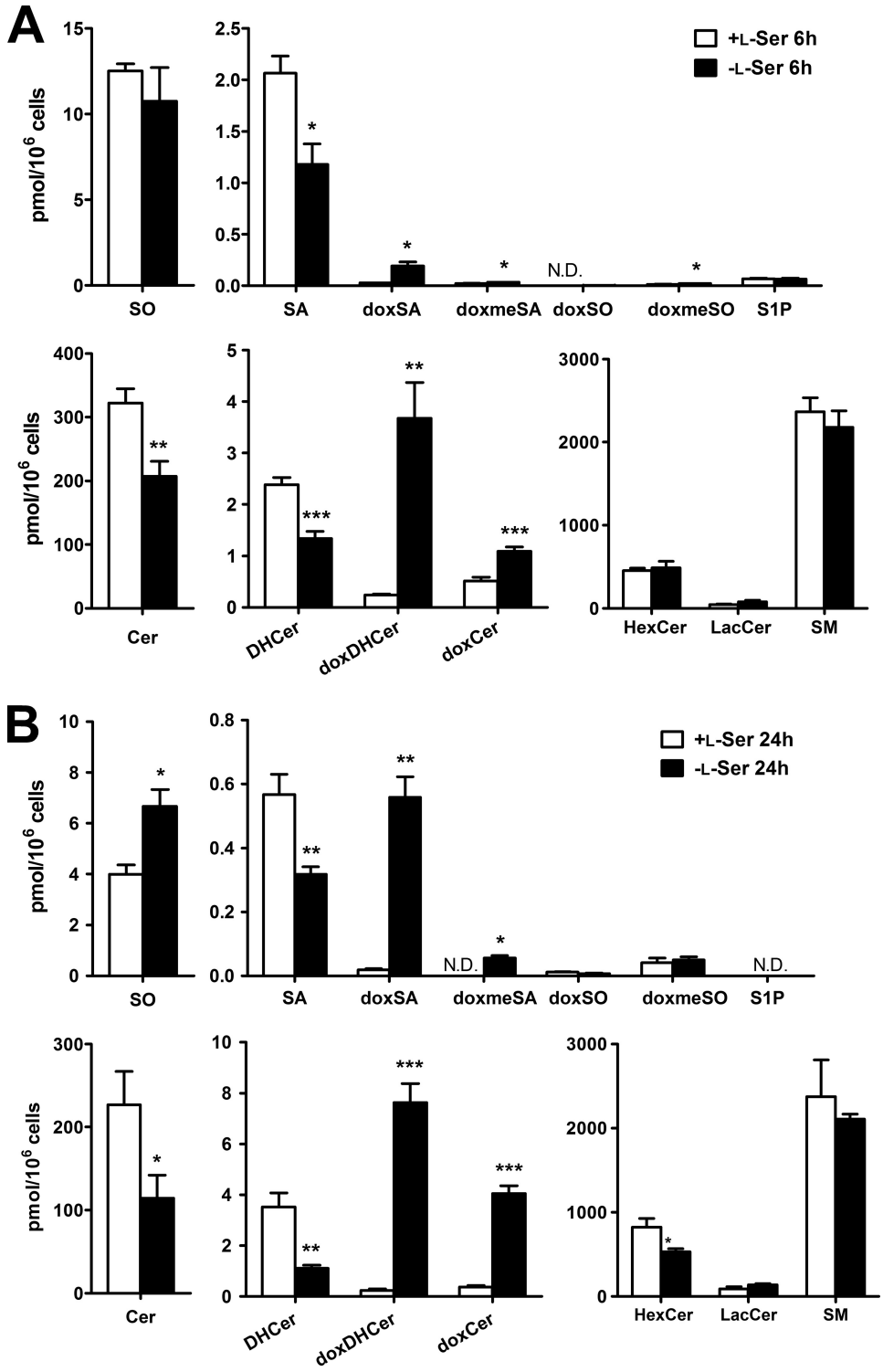

FIGURE 3. **Induction of doxSLs in KO-MEFs because of L-Ser deprivation.** KO-MEFs were cultured under L-Ser-supplemented or -deprived conditions for 6 h (*A*) or 24 h (*B*). Then, extracted lipids were analyzed using LC-MS. The data are means ± S.E. from more than three independent experiments. The differences between the two groups were analyzed using the Student's *t* test (*, $p < 0.05$; **, $p < 0.01$; ***, $p < 0.001$). *S1P*, sphingosine 1-phosphate; *N.D.*, not detected.

Despite the presence of L-Ser, the addition of 5 μM doxSA caused a drastic reduction of viable KO-MEF cell numbers after 24 h of incubation (Fig. 9*A*). Unlike doxSA, SA, a normal sphingoid base, did not affect the viability and cell proliferation of KO-MEFs when added at a concentration of 5 μM (Fig. 9*A*). Suppression of proliferation was evident between 24 and 48 h in KO-MEFs treated with 1 μM doxSA (Fig. 9*B*), whereas no significant effect on KO-MEF proliferation was observed by treatment with doxSA at 0.01 or 0.1 μM (Fig. 9*B*). Similar to KO-MEFs, the addition of more than 1 μM doxSA under L-Ser-supplemented culture conditions suppressed cell proliferation of WT-MEFs, despite their ability to synthesize L-Ser through

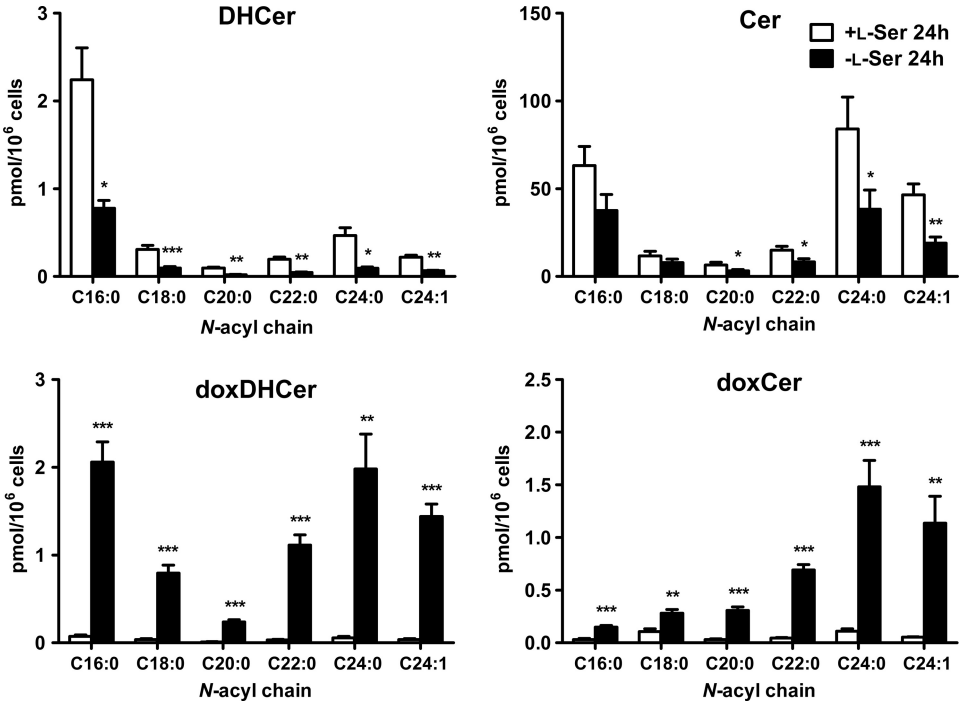

FIGURE 4. **Fatty acid composition of four ceramide species present in KO-MEFs after L-Ser deprivation for 24 h.** KO-MEFs were cultured under L-Ser-supplemented or -deprived conditions for 24 h. Then, extracted lipids were analyzed using LC-MS. The data are means ± S.E. (+*L-Ser*, $n = 5$; −*L-Ser*, $n = 8$). The differences between the two groups were analyzed using the Student's *t* test (*, $p < 0.05$; **, $p < 0.01$; ***, $p < 0.001$).

Phgdh (Fig. 9*C*). In HeLa cells, treatment with doxSA at 5 μM also caused a gradual reduction in viable cell number over time, whereas the cells were able to proliferate after treatment with 1 μM doxSA (Fig. 9*D*). The fact that KO-MEFs and WT-MEFs tended to be more sensitive to doxSA toxicity than HeLa cells indicates that there are significant differences among cell types with respect to resistance to doxSA cytotoxicity.

L-Serine Deficiency Induced Lipid Body Formation in KO-MEFs—We next investigated morphological changes of KO-MEFs between L-Ser-supplemented and L-Ser-deprived conditions. As shown in Fig. 10*A*, in bright field microscopy, bright structures were observed under the L-Ser-deprived conditions. Those structures were clearly stained with Nile Red, indicating that they were lipid bodies (Fig. 10*A*). Transmission electron microscopic analysis showed that formed lipid bodies had lamellar inclusions (Fig. 10*B*, *arrows*). To assess whether doxSLs associate with lipid bodies induced by the L-Ser-deprived condition, we performed lipid analysis of lipid bodies in KO-MEFs by LC-MS. The lipid bodies in L-Ser-deprived condition exhibited a drastic increase in doxSLs (doxDHCer and doxCer) and a significant decrease in normal sphingolipids (Cer, DHCer, SM, and HexCer) compared with L-Ser-supplemented conditions (Fig. 10*C*). These results suggest that highly hydrophobic doxSLs synthesized under L-Ser-deprived conditions accumulated in the lipid bodies of KO-MEFs.

Discussion

This study demonstrated, for the first time, that reduced availability of L-Ser triggers the synthesis of doxSLs in cultured cells and the brain, and an influx of L-Ala into the sphingolipid synthetic pathway becomes evident in cells when the ratio of L-Ala to L-Ser reaches above 3.0 (Table 3). These results indicate that doxSLs are generated under conditions of imbalance between L-Ala and L-Ser in nonmalignant cells and tissues, suggesting a possible role of doxSLs in the pathobiology of L-Ser deficiency disorders and other diseases involving an increased ratio of L-Ala to L-Ser in serum and/or tissues.

In addition to doxSA generation, this study demonstrated that the reduced availability of L-Ser led to different respective changes of the major sphingolipid species in KO-MEFs. Marked decreases in DHCer, Cer, and HexCer occurred simultaneously under L-Ser deprivation, although no such significant or marked changes were seen in SM, the most abundant SL species, and LacCer (Fig. 3). A recent study also reported that siRNA knockdown of ceramide synthase resulted in complex changes in the levels of Cer and other SLs in a breast cancer cell line, MCF-7 (26). Ceramide synthase 2 is a predominant ceramide synthase species in the cell, and its knockdown resulted in a decrease in Cer containing C22-C24 saturated and monounsaturated fatty acids, although parallel decreases in HexCer, LacCer, and SM containing very long acyl chains were not observed. Instead, ceramide synthase 2 knockdown increased Cer, HexCer, and LacCer containing C14-C18 fatty acids (26). These observations, together with our findings, suggest that the steady-state levels of individual SL species are maintained in cells by as-yet-unknown multiple regulatory mechanisms. Furthermore, it seems likely that maintaining the mass of some particular SL species may be an adaptive response of cells to conditions of L-Ser and/or Cer deficiency.

Among doxSLs, doxSA was initially discovered as an antitumor compound, spisulosine/ES-285, from the marine clam *Spisula polynyma* (25). Purified doxSA can induce rearrangement of actin stress fibers (25) and cause apoptosis and sup-

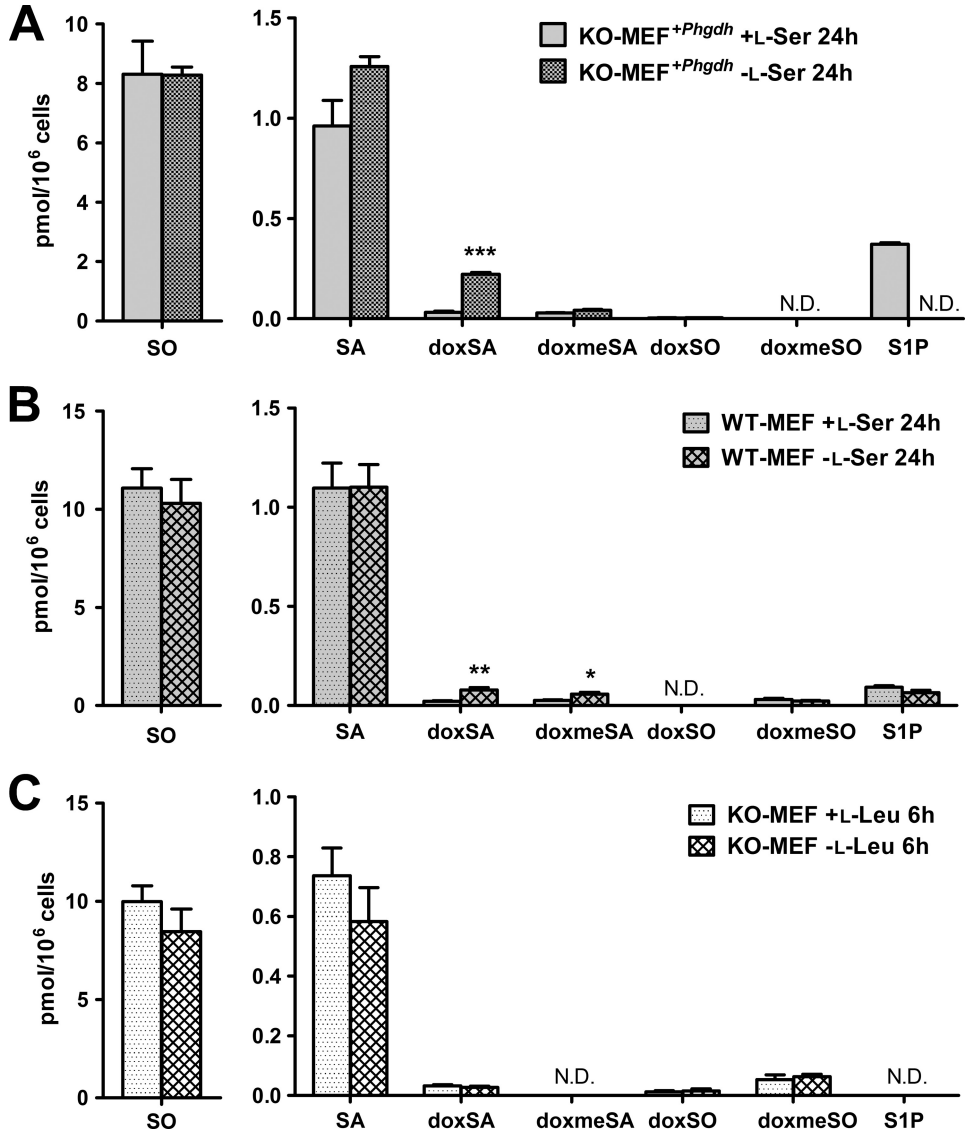

FIGURE 5. **Suppression of doxSL production in MEFs expressing transduced *Phgdh*.** KO-MEFs expressing *Phgdh* (retroviral transduction) (*A*) or WT-MEFs (*B*) were cultured under L-Ser-supplemented or -deprived conditions for 24 h. *C*, KO-MEFs were cultured under L-Leu-supplemented or -deprived conditions for 6 h. Then, lipids were extracted and analyzed using LC-MS. The data are means ± S.E. (KO-MEFs expressing *Phgdh* and KO-MEFs −*L-Leu*, $n = 4$; WT-MEFs, $n = 6$; KO-MEFs +*L-Leu*, $n = 5$). Differences between the two groups were analyzed using the Student's *t* test (*, $p < 0.05$; **, $p < 0.01$; ***, $p < 0.001$). *N.D.*, not detected; *S1P*, sphingosine 1-phosphate.

pression of cancer cell proliferation (24). However, in a phase I trial of doxSA conducted in patients with advanced solid tumors, doxSA showed poor antitumor activity and caused many adverse reactions, including mild-to-moderate nausea, pyrexia, injection site reactions, and vomiting (27–29). In addition, some patients developed neuropathy and liver damage (27–29). Thus, these results provide clinical evidence that, at high doses, doxSA causes tissue damage. Consistent with these observations, doxSA exhibited more intense cytotoxic effects on KO-MEFs and WT-MEFs than HeLa cells.

In mammals, doxSLs was first found in tissues and cultured cells (LLC-PK_1, Vero, J774, HT29, and HEK293) treated with fumonisin B_1, a carcinogenic and toxic mycotoxin that inhibits ceramide synthases that catalyze acylation of sphingoid bases, including sphinganine (21). In these fumonisin B_1-treated cells, the synthesis of doxSLs requires SPT. In this study, we demonstrated that among the doxSLs, doxSA and doxDHCer were the major species present in cultured cells and in mouse tissues lacking *Phgdh*-dependent L-Ser synthesis. These findings indicated that L-Ala can be utilized endogenously as a substrate of SPT in various cells and tissues when ceramide synthesis is inhibited. Thus, our present observations coincide well with the findings reported by Zitomer *et al.* (21) and highlight the causative roles for reduced L-Ser availability as well as disturbed ceramide synthesis in the generation of doxSLs. Sphingoid bases of doxSLs are also found in plasma of patients with hereditary sensory and autonomic neuropathy (HSAN1) (30, 31). Genetic studies revealed that missense mutations in the *SPTLC1* or *SPTLC2* subunit of SPT are responsible for HSAN1; SPT with HSAN1 mutations starts to use L-Ala and Gly as substrates and can synthesize doxSLs (30, 31). An enzyme kinetics study of SPT showed that wild-type SPT has a higher affinity and a higher V_{max} value for L-Ser compared with the HSAN1 mutant (30). Instead, the HSAN1 mutant enzyme acquires an

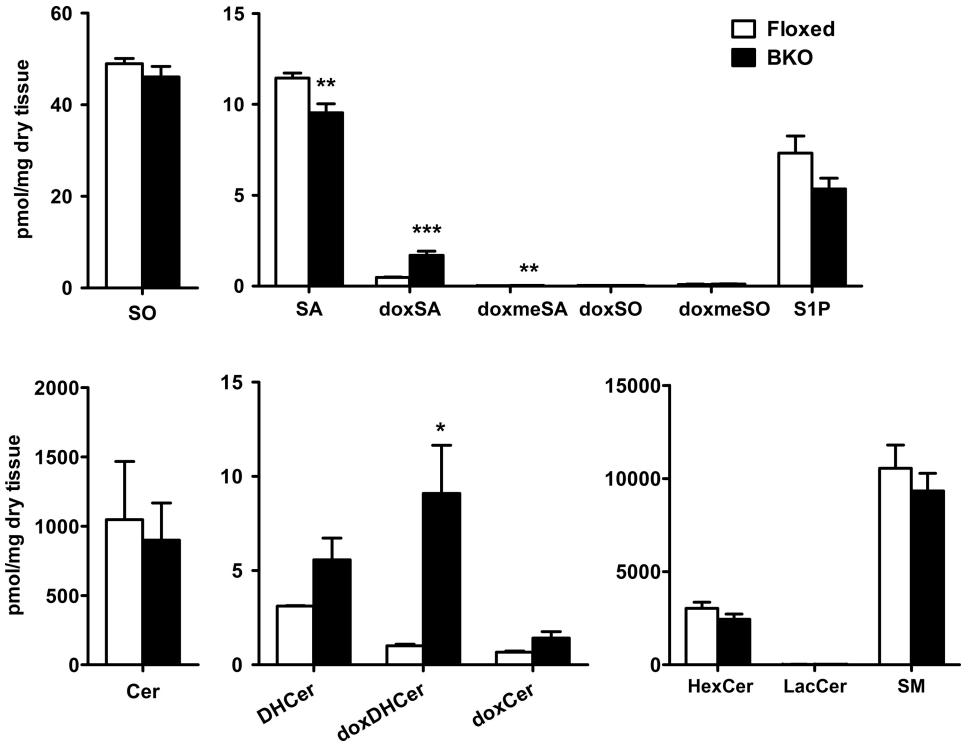

FIGURE 6. **Production of doxSLs in the brain of BKO mice.** Lipids were extracted from brain homogenates and analyzed using LC-MS. The data are means ± S.E. (floxed, $n = 7$; BKO, $n = 8$). Differences between the two groups were analyzed using the Student's *t* test (*, $p < 0.05$; **, $p < 0.01$; ***, $p < 0.001$).

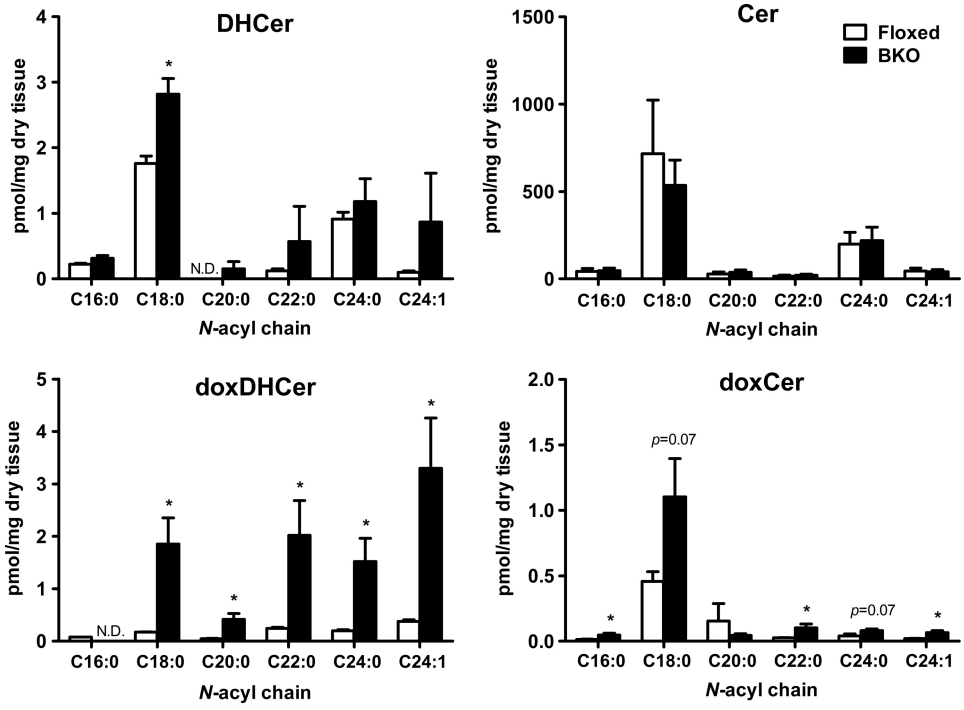

FIGURE 7. **Fatty acid profile of *N*-acyl derivatives present in the brains of BKO and control (floxed) mice.** Lipids were extracted from brain homogenates and analyzed using LC-MS. The data are means ± S.E. (floxed, $n = 7$; BKO, $n = 8$). Differences between the two groups were analyzed using the Student's *t* test (*, $p < 0.05$; **, $p < 0.01$; ***, $p < 0.001$). *N.D.*, not detected.

affinity for L-Ala. In sharp contrast to the mutant, the wild-type SPT does not efficiently utilize L-Ala in the assay conditions used, precluding the direct measurement K_m values (30). However, the K_i values for L-Ala of the wild-type and mutant SPT appear to be of similar magnitude, also indicating that L-Ala is capable of interacting with the substrate-binding domain of both SPT forms (30).

Patients with diabetes often exhibit progressive sensory neuropathy, which has clinical similarities to that observed in HSAN1 patients. Recent biochemical studies reported

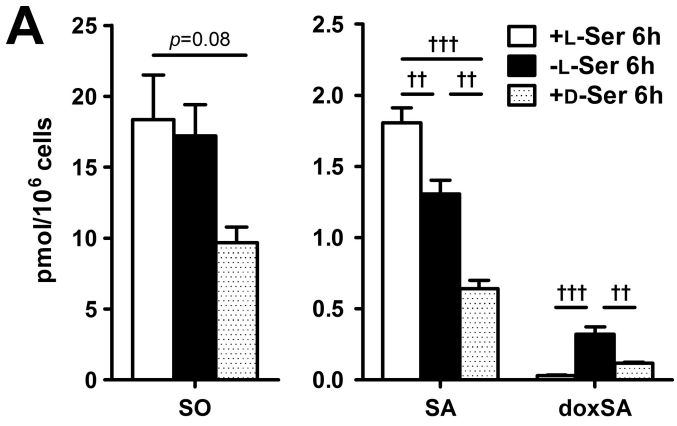

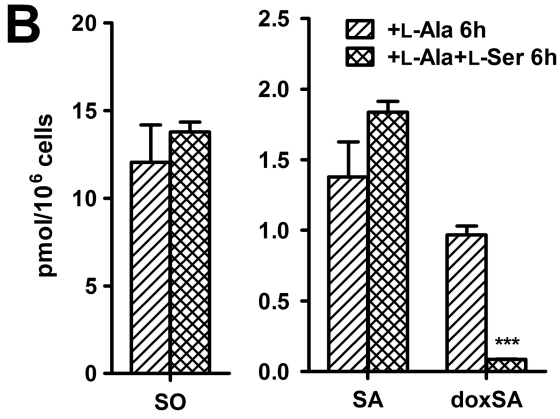

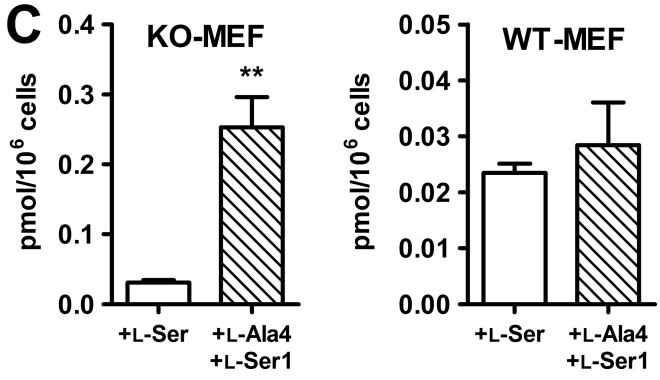

FIGURE 8. **Effect of D-Ser or L-Ala treatment on the synthesis of sphingoid bases in KO-MEFs.** *A,* KO-MEFs were cultured for 6 h in EMEM supplemented with 400 μM L-Ser, 400 μM D-Ser, or under the same culture condition without any of the above supplementations (*i.e.* L-Ser-deprived cells). *B,* KO-MEFs maintained for 6 h under conditions supplemented with 400 μM L-Ala or 400 μM L-Ser with 400 μM L-Ala. *C,* MEFs were cultured for 6 h (KO-MEFs, *left*) or 24 h (WT-MEFs, *right*) in EMEM supplemented with 400 μM L-Ser or 400 μM L-Ala with 100 μM L-Ser. Then, lipids were extracted and analyzed using LC-MS. The data are means ± S.E. (+*L-Ser*, −*L-Ser*, *L-Ala* and +*L-Ala-4* + *L-Ser-1*, $n = 5$; +*D-Ser*, $n = 4$; +*L-Ala* + *L-Ser*, $n = 6$). Differences were analyzed using one-way analysis of variance followed by the Tukey-Kramer test (††, $p < 0.01$; †††, $p < 0.001$). Differences between the two groups were analyzed using the Student's *t* test (**, $p < 0.01$; ***, $p < 0.001$).

TABLE 3
Amino acid concentrations and doxSA contents in the MEFs

MEFs	Medium	Culture time	Ala[a]	Ser[a]	Ala/Ser	doxSA production[b]
		h				
WT	+L-Ser	6	2.72	6.39	0.4	−
	−L-Ser		2.33	4.44	0.5	−
KO	+L-Ser		3.24	2.84	1.1	1.0
	−L-Ser		3.25	0.98	3.3	10.3
WT	+L-Ser	24	5.64	4.45	1.3	0.7
	−L-Ser		5.51	3.46	1.6	2.5
KO	+L-Ser		3.88	1.84	2.1	0.6
	−L-Ser		3.00	0.82	3.7	18.0

[a] Intracellular amino acid concentrations (nmol/10^9 cells) are shown as means ($n = 3$).
[b] The amounts of doxSA in WT or KO-MEFs in each condition shown in Fig. 3 were normalized to that obtained from KO-MEFs maintained under the L-Ser-supplemented condition for 6 h. −, not determined.

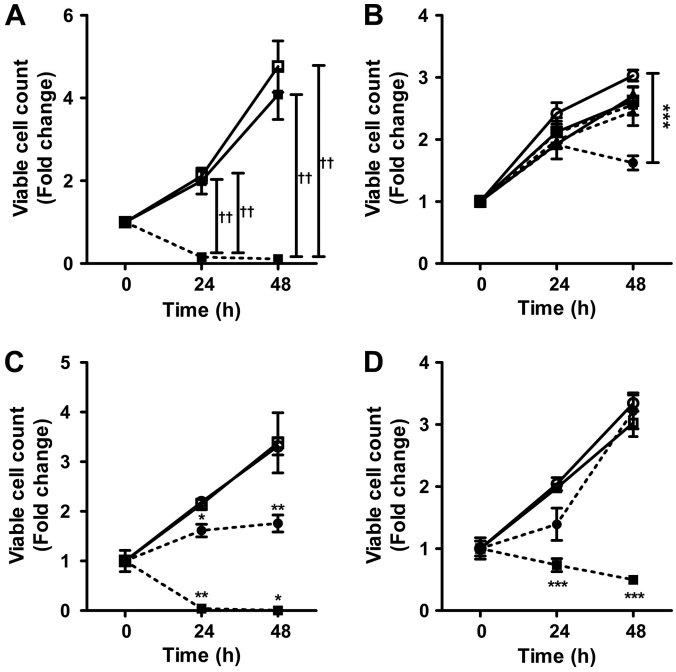

FIGURE 9. **Effect of doxSA on KO-MEFs, WT-MEFs, and HeLa cells.** KO-MEFs (*A* and *B*), WT-MEFs (*C*), or HeLa (*D*) cells were cultured for up to 48 h in a medium containing 400 μM L-Ser with either SA (5 μM) or doxSA (0.01, 0.1, 1, or 5 μM). *A,* viable cell numbers of KO-MEFs treated with 5 μM SA (*solid line* with *closed squares*), 5 μM doxSA (*dotted line* with *closed squares*), and the vehicle control (*open squares*) in the presence of L-Ser. *B,* viable cell numbers of KO-MEFs treated with 0.01 μM (*closed squares*), 0.1 μM (*closed triangles*), and 1 μM (*closed circles*) of doxSA in the presence of L-Ser. The *open symbols* show viable cell numbers of KO-MEFs treated with the corresponding concentration of vehicle control in the presence of L-Ser. *C* and *D,* proliferation of WT-MEFs (*C*) or HeLa (*D*) cells treated with 1 μM (*closed circles*) and 5 μM doxSA (*closed diamonds*). The *open symbols* show viable cell numbers of cells treated with the corresponding concentration of vehicle control in the presence of L-Ser. Cell viability was assessed using the trypan blue exclusion method. The data are means ± S.E. from three independent experiments. Differences were analyzed using one-way analysis of variance followed by the Tukey-Kramer test (††, $p < 0.01$). Differences between the two groups were analyzed using the Student's *t* test (*, $p < 0.05$; **, $p < 0.01$; ***, $p < 0.001$).

increased doxSL levels and a concomitant decrease in the L-Ser content or increase in the L-Ala content in the plasma of patients with type II diabetes and metabolic syndrome (32–35) (Table 4). Previous studies also showed that an increased L-Ala level and a simultaneously decreased L-Ser level in plasma and tissues are associated with experimental diabetes in mice and rats (Table 4) (36, 37). Therefore, further studies will be necessary to elucidate a structural basis for L-Ala recognition by SPT to prevent doxSL generation in these diseases.

HSAN1 patients usually present with peripheral sensory neuropathy but show no signs or symptoms in the central nervous system (CNS). Elevated levels of doxSLs are also found in the peripheral nervous system, but not in the CNS, of *SPTLC1* C133W mutant mice (38, 39). L-Ser is abundantly synthesized via the phosphorylated pathway that is active in astrocytes in

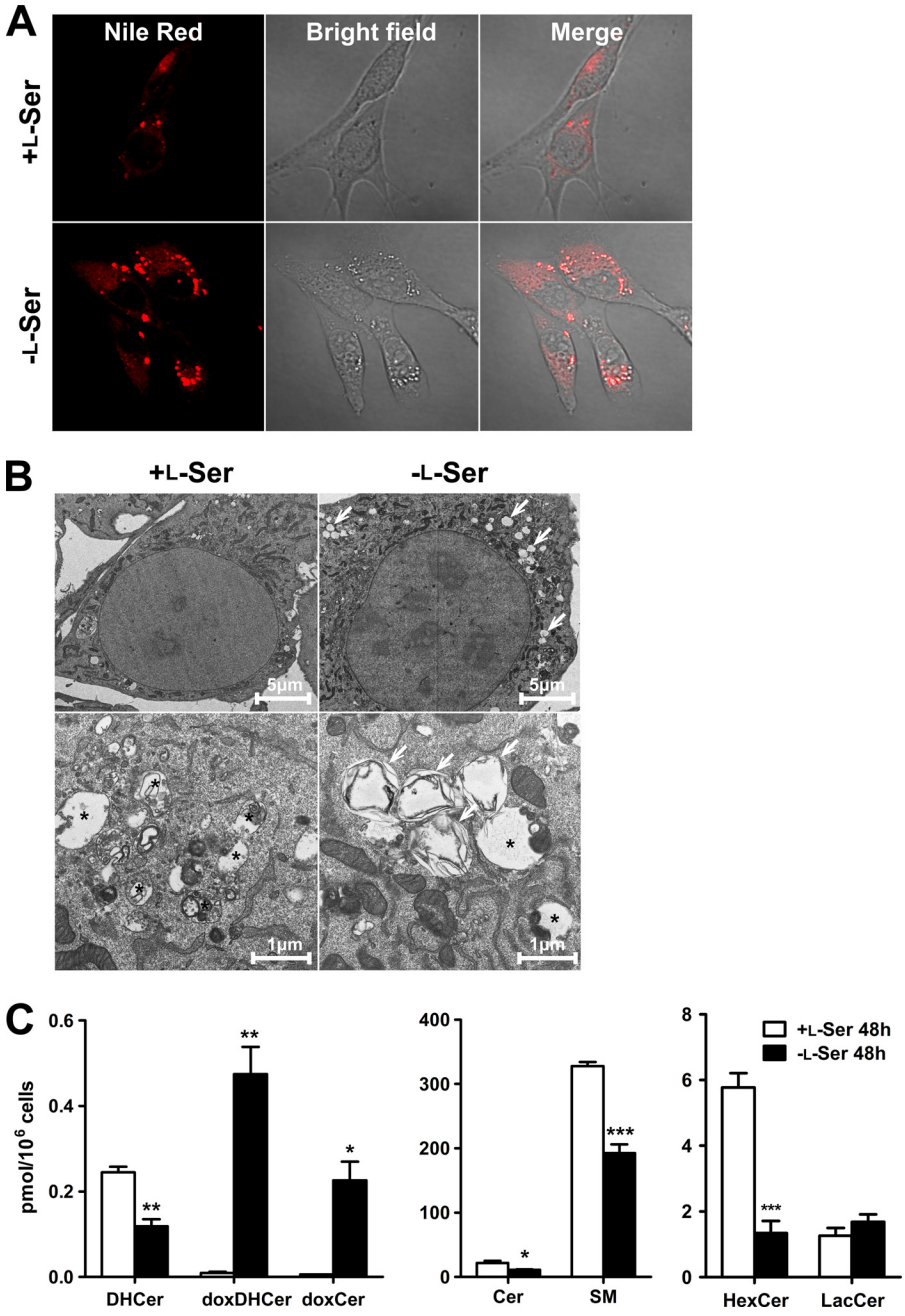

FIGURE 10. **Lipid body formation in KO-MEFs induced by L-Ser deficiency.** KO-MEFs were cultured under L-Ser-supplemented or -deprived conditions for 24 h (*B*) or 48 h (*A* and *C*). *A,* lipid bodies were stained with Nile Red and observed under a confocal microscope. *B,* after incubation, KO-MEFs were fixed and observed under an electron microscope. In L-Ser-deprived group, lipid bodies having lamellar inclusions increased (*arrows*). *Asterisk* indicates autophagosomes. *C,* following incubation of KO-MEFs for 48 h, lipids extracted from lipid bodies were analyzed using LC-MS. The data are means ± S.E. (+L-*Ser*, $n = 3$; −L-*Ser*, $n = 4$). The differences between the two groups were analyzed using the Student's *t* test (*, $p < 0.05$; **, $p < 0.01$; ***, $p < 0.001$).

TABLE 4
Increased ratio of Ala to Ser in diabetes

		Ala/Ser		
	Sample	Control	diabetes	Refs.
Rat (alloxan-diabetic)	Heart	2.3	6.2	Scharff and Wool (36)
	Plasma	1.4	2.7	
Rat (pancreatectomized)	Heart	4.4	8.4	
	Plasma	1.2	1.4	
Rat (anti-insulin treated)	Heart	2.2	3.1	
	Plasma	1.3	1.5	
Human (type II)	Platelet	1.3	1.8	De Luca *et al.* (32)
Human (type II)	Plasma	2.7	3.0	Bertea *et al.* (33)
Human (metabolic syndrome)	Plasma	2.8	3.4	Kamaura *et al.* (50)

the CNS (11, 40). Indeed, published and unpublished observations in our laboratory showed that the free L-Ser content in the hippocampus of mice (~350 nmol/g tissue) does not differ substantially from the L-Ala content (~550 nmol/g tissue). In contrast, the L-Ala concentration in serum (approximately >300 μM) is much higher than the L-Ser concentration (approximately <100 μM) in mice (11).[5] Similar profiles of L-Ala and L-Ser concentrations occur in human sera (33). Therefore, despite the high affinity of mutant SPT for L-Ala, only peripheral neurons of HSAN1 patients and model mice carrying the HSAN1 mutation are able to use L-Ala to synthesize doxSLs. Thus, tissue damage caused by doxSLs seems to occur more frequently in the peripheral nervous system than in the CNS of patients with HSAN1. In addition, we found that the addition of D-Ser suppressed the production of both normal SLs and doxSLs. These findings open up the possibility that doxSL production in the CNS is protected by D-Ser in the healthy adult brain because D-Ser is present at high levels (~30% of total Ser) in the mammalian adult brain (11, 22, 40). Nevertheless, doxSLs occurred in the brain of BKO mice. Because the free L-Ser level in the BKO brain drops substantially (11, 40), a high L-Ala/L-Ser ratio and a simultaneous decrease in D-Ser because of the genetic inactivation of *Phgdh* are the most likely causes of the accumulation of doxSLs in the BKO brain.

Lipid droplets, which are a kind of lipid bodies, are ubiquitous and dynamic organelles that serve as reservoirs of lipids for energy metabolism, membrane synthesis, and generation of important lipid-derived molecules. Lipid droplets, which are known to consist of mainly triacylglycerols and sterol esters, are formed at the endoplasmic reticulum (ER) (41). In addition, it is likely that lipid droplets operate to defend cells against lipotoxicity by storing hydrophobic lipid molecules. The formation of lipid droplets is also elicited under ER stress (42). SPT, a rate-limiting enzyme in the sphingolipid synthetic pathway, is localized mainly in the ER, and *de novo* synthesis of SA, DHCer, and Cer occurs in the ER (13, 43). Thus, sphingolipids synthesized in the ER can participate in lipid body formation. This study demonstrated that L-Ser-deprived conditions induced the generation of doxSLs and the formation of lipid bodies in KO-MEFs. doxSLs, which increased under L-Ser-deprived conditions, accumulated in lipid bodies of KO-MEFs. These results raise the possibility that highly hydrophobic and poorly metabolized doxSLs, such as doxDHCer and doxCer, are sequestered in lipid bodies to suppress lipotoxicity. Intriguingly, increased numbers of lipid droplets were also observed in the HSAN1 patient-derived lymphoblasts (44). Therefore, doxSLs may accumulate in the lipid droplets of HSAN1 lymphoblasts as seen in KO-MEFs.

Recently, it was proposed that enhanced synthesis of L-Ser via the phosphorylated pathway in cancer cells supports metabolic reprogramming such as aerobic glycolysis and lactate production through activation of pyruvate kinase M2, which provides metabolic advantages to cancer cells in terms of growth and survival (10, 45, 46). These observations have led to an idea of chemical or genetic suppression of *PHGDH*, *PSAT1*, or *PSPH* in the phosphorylated pathway of L-Ser synthesis as a potential new anticancer treatment. It is quite possible, however, that inhibition of *de novo* L-Ser synthesis leads to an increase in the ratio of L-Ala to L-Ser, which can have negative effects on healthy cells and tissues through up-regulation of doxSL synthesis. Therefore, preventing doxSL production may be a key factor that will determine whether modulating the expression of enzymes involved in *de novo* L-Ser synthesis is suitable for cancer therapy.

The *N*-acylation of SA in mammals is catalyzed by ceramide synthases, which are a family of six enzymes (47). Each ceramide synthase has a high specificity toward the acyl-CoA chain length used for the *N*-acylation. In addition, the introduction of the 4,5-*trans*-double bond in the sphingoid backbone of SLs occurs at the level of DHCer via a dihydroceramide desaturase (48). The distribution of ceramide synthases and dihydroceramide desaturase differs among different cells and tissues (47, 49). Thus, these enzymes are responsible for the fatty acid compositions of SLs in a tissue- and cell-specific manner. In this study, doxDHCer was the most abundant species in KO-MEFs and the mature brain (Figs. 3 and 6). Because fumonisin B_1 blocked the synthesis of doxDHCer in a variety of culture cells (21), ceramide synthases seem to be the likely enzymes involved in the *N*-acylation of doxSLs under L-Ser-deprived conditions. Unlike usual SLs, the major compositions of doxSLs are long chain fatty acids such as C22:0, C24:0, or C24:1. If ceramide synthase catalyzes the *N*-acylation of doxSA as in normal SLs, it is plausible that each enzyme has a different affinity to doxSA. Furthermore, our findings suggest that enzymes catalyzing the synthesis of long chain SLs have a higher affinity to doxSLs than enzymes synthesizing short chain SLs.

Although doxSA is capable of activating several cellular signaling cascades[4] (33), cellular targets of doxSLs, including doxSA and doxDHCer, remain largely unexplored. Thus, understanding of molecular interactions between doxSLs and cellular components, and their consequences, is expected to facilitate the development of therapeutic strategies against the cellular damage evoked by L-Ser deficiency and other metabolic disorders.

Acknowledgments—We thank Dr. Yoko Ohashi (RIKEN), Dr. Takemichi Nakamura (Molecular Characterization Team, RIKEN), and Dr. Shota Sakai (Frontier Research Center for Post-genome Science and Technology, Hokkaido University) for valuable technical advice and help with mass spectrometric analysis; Prof. Makoto Ito (Department of Bioscience and Biotechnology, Graduate School of Bioresource and Bioenvironmental Sciences, Kyushu University) for valuable technical advice of the isolation of lipid bodies; and Dr. Tetsuo Ohnishi (Laboratory for Molecular Psychiatry, RIKEN) and Dr. Peter Greimel (Lipid Biology Laboratory, RIKEN) for their critical reading of the manuscript.

[5] K. Esaki, Y. Hirabayashi, and S. Furuya, unpublished observations.

References

1. Ichihara, A., and Greenberg, D. M. (1955) Pathway of serine formation from carbohydrate in rat liver. *Proc. Natl. Acad. Sci. U.S.A.* **41,** 605–609
2. Snell, K. (1984) Enzymes of serine metabolism in normal, developing and neoplastic rat tissues. *Adv. Enzyme Regul.* **22,** 325–400
3. de Koning, T. J., Duran, M., Dorland, L., Gooskens, R., Van Schaftingen, E.,

Jaeken, J., Blau, N., Berger, R., and Poll-The, B. T. (1998) Beneficial effects of L-serine and glycine in the management of seizures in 3-phosphoglycerate dehydrogenase deficiency. *Ann. Neurol.* **44,** 261–265
4. de Koning, T. J., Klomp, L. W., van Oppen, A. C., Beemer, F. A., Dorland, L., van den Berg, I., and Berger, R. (2004) Prenatal and early postnatal treatment in 3-phosphoglycerate-dehydrogenase deficiency. *Lancet* **364,** 2221–2222
5. Klomp, L. W., de Koning, T. J., Malingré, H. E., van Beurden, E. A., Brink, M., Opdam, F. L., Duran, M., Jaeken, J., Pineda, M., Van Maldergem, L., Poll-The, B. T., van den Berg, I. E., and Berger, R. (2000) Molecular characterization of 3-phosphoglycerate dehydrogenase deficiency–a neurometabolic disorder associated with reduced L-serine biosynthesis. *Am. J. Hum. Genet.* **67,** 1389–1399
6. Mitoma, J., Furuya, S., Shimizu, M., Shinoda, Y., Yoshida, K., Azuma, N., Tanaka, H., Suzuki, Y., and Hirabayashi, Y. (2004) Mouse 3-phosphoglycerate dehydrogenase gene: genomic organization, chromosomal localization, and promoter analysis. *Gene* **334,** 15–22
7. Yoshida, K., Furuya, S., Osuka, S., Mitoma, J., Shinoda, Y., Watanabe, M., Azuma, N., Tanaka, H., Hashikawa, T., Itohara, S., and Hirabayashi, Y. (2004) Targeted disruption of the mouse 3-phosphoglycerate dehydrogenase gene causes severe neurodevelopmental defects and results in embryonic lethality. *J. Biol. Chem.* **279,** 3573–3577
8. Kawakami, Y., Yoshida, K., Yang, J. H., Suzuki, T., Azuma, N., Sakai, K., Hashikawa, T., Watanabe, M., Yasuda, K., Kuhara, S., Hirabayashi, Y., and Furuya, S. (2009) Impaired neurogenesis in embryonic spinal cord of Phgdh knockout mice, a serine deficiency disorder model. *Neurosci. Res.* **63,** 184–193
9. Possemato, R., Marks, K. M., Shaul, Y. D., Pacold, M. E., Kim, D., Birsoy, K., Sethumadhavan, S., Woo, H. K., Jang, H. G., Jha, A. K., Chen, W. W., Barrett, F. G., Stransky, N., Tsun, Z. Y., Cowley, G. S., *et al.* (2011) Functional genomics reveal that the serine synthesis pathway is essential in breast cancer. *Nature* **476,** 346–350
10. Chaneton, B., Hillmann, P., Zheng, L., Martin, A. C., Maddocks, O. D., Chokkathukalam, A., Coyle, J. E., Jankevics, A., Holding, F. P., Vousden, K. H., Frezza, C., O'Reilly, M., and Gottlieb, E. (2012) Serine is a natural ligand and allosteric activator of pyruvate kinase M2. *Nature* **491,** 458–462
11. Yang, J. H., Wada, A., Yoshida, K., Miyoshi, Y., Sayano, T., Esaki, K., Kinoshita, M. O., Tomonaga, S., Azuma, N., Watanabe, M., Hamase, K., Zaitsu, K., Machida, T., Messing, A., Itohara, S., *et al.* (2010) Brain-specific Phgdh deletion reveals a pivotal role for L-serine biosynthesis in controlling the level of D-serine, an *N*-methyl-D-aspartate receptor co-agonist, in adult brain. *J. Biol. Chem.* **285,** 41380–41390
12. Hannun, Y. A., and Obeid, L. M. (2008) Principles of bioactive lipid signalling: lessons from sphingolipids. *Nat. Rev. Mol. Cell Biol.* **9,** 139–150
13. Pitson, S. M. (2011) Regulation of sphingosine kinase and sphingolipid signaling. *Trends Biochem. Sci.* **36,** 97–107
14. Lowther, J., Naismith, J. H., Dunn, T. M., and Campopiano, D. J. (2012) Structural, mechanistic and regulatory studies of serine palmitoyltransferase. *Biochem. Soc. Trans.* **40,** 547–554
15. Sayano, T., Kawakami, Y., Kusada, W., Suzuki, T., Kawano, Y., Watanabe, A., Takashima, K., Arimoto, Y., Esaki, K., Wada, A., Yoshizawa, F., Watanabe, M., Okamoto, M., Hirabayashi, Y., and Furuya, S. (2013) L-Serine deficiency caused by genetic Phgdh deletion leads to robust induction of 4E-BP1 and subsequent repression of translation initiation in the developing central nervous system. *FEBS J.* **280,** 1502–1517
16. Ogawa, T., Ishida-Kitagawa, N., Tanaka, A., Matsumoto, T., Hirouchi, T., Akimaru, M., Tanihara, M., Yogo, K., and Takeya, T. (2006) A novel role of L-serine (L-Ser) for the expression of nuclear factor of activated T cells (NFAT)2 in receptor activator of nuclear factor κB ligand (RANKL)-induced osteoclastogenesis *in vitro*. *J. Bone Miner. Metab.* **24,** 373–379
17. Morita, S., Kojima, T., and Kitamura, T. (2000) Plat-E: an efficient and stable system for transient packaging of retroviruses. *Gene Ther.* **7,** 1063–1066
18. Ding, Y., Zhang, S., Yang, L., Na, H., Zhang, P., Zhang, H., Wang, Y., Chen, Y., Yu, J., Huo, C., Xu, S., Garaiova, M., Cong, Y., and Liu, P. (2013) Isolating lipid droplets from multiple species. *Nat. Protoc.* **8,** 43–51
19. Shaner, R. L., Allegood, J. C., Park, H., Wang, E., Kelly, S., Haynes, C. A., Sullards, M. C., and Merrill, A. H., Jr. (2009) Quantitative analysis of sphingolipids for lipidomics using triple quadrupole and quadrupole linear ion trap mass spectrometers. *J. Lipid Res.* **50,** 1692–1707
20. Merrill, A. H., Jr., Sullards, M. C., Allegood, J. C., Kelly, S., and Wang, E. (2005) Sphingolipidomics: high-throughput, structure-specific, and quantitative analysis of sphingolipids by liquid chromatography tandem mass spectrometry. *Methods* **36,** 207–224
21. Zitomer, N. C., Mitchell, T., Voss, K. A., Bondy, G. S., Pruett, S. T., Garnier-Amblard, E. C., Liebeskind, L. S., Park, H., Wang, E., Sullards, M. C., Merrill, A. H., Jr., and Riley, R. T. (2009) Ceramide synthase inhibition by fumonisin B1 causes accumulation of 1-deoxysphinganine: a novel category of bioactive 1-deoxysphingoid bases and 1-deoxydihydroceramides biosynthesized by mammalian cell lines and animals. *J. Biol. Chem.* **284,** 4786–4795
22. Wolosker, H., Dumin, E., Balan, L., and Foltyn, V. N. (2008) D-Amino acids in the brain: D-serine in neurotransmission and neurodegeneration. *FEBS J.* **275,** 3514–3526
23. Hanada, K., Hara, T., and Nishijima, M. (2000) D-Serine inhibits serine palmitoyltransferase, the enzyme catalyzing the initial step of sphingolipid biosynthesis. *FEBS Lett.* **474,** 63–65
24. Salcedo, M., Cuevas, C., Alonso, J. L., Otero, G., Faircloth, G., Fernandez-Sousa, J. M., Avila, J., and Wandosell, F. (2007) The marine sphingolipid-derived compound ES 285 triggers an atypical cell death pathway. *Apoptosis* **12,** 395–409
25. Cuadros, R., Montejo de Garcini, E., Wandosell, F., Faircloth, G., Fernández-Sousa, J. M., and Avila, J. (2000) The marine compound spisulosine, an inhibitor of cell proliferation, promotes the disassembly of actin stress fibers. *Cancer Lett.* **152,** 23–29
26. Mullen, T. D., Spassieva, S., Jenkins, R. W., Kitatani, K., Bielawski, J., Hannun, Y. A., and Obeid, L. M. (2011) Selective knockdown of ceramide synthases reveals complex interregulation of sphingolipid metabolism. *J. Lipid Res.* **52,** 68–77
27. Baird, R. D., Kitzen, J., Clarke, P. A., Planting, A., Reade, S., Reid, A., Welsh, L., López Lázaro, L., de las Heras, B., Judson, I. R., Kaye, S. B., Eskens, F., Workman, P., deBono, J. S., and Verweij, J. (2009) Phase I safety, pharmacokinetic, and pharmacogenomic trial of ES-285, a novel marine cytotoxic agent, administered to adult patients with advanced solid tumors. *Mol. Cancer Ther.* **8,** 1430–1437
28. Schöffski, P., Dumez, H., Ruijter, R., Miguel-Lillo, B., Soto-Matos, A., Alfaro, V., and Giaccone, G. (2011) Spisulosine (ES-285) given as a weekly three-hour intravenous infusion: results of a phase I dose-escalating study in patients with advanced solid malignancies. *Cancer Chemother. Pharmacol.* **68,** 1397–1403
29. Massard, C., Salazar, R., Armand, J. P., Majem, M., Deutsch, E., García, M., Oaknin, A., Fernández-García, E. M., Soto, A., and Soria, J. C. (2012) Phase I dose-escalating study of ES-285 given as a three-hour intravenous infusion every three weeks in patients with advanced malignant solid tumors. *Invest. New Drugs* **30,** 2318–2326
30. Gable, K., Gupta, S. D., Han, G., Niranjanakumari, S., Harmon, J. M., and Dunn, T. M. (2010) A disease-causing mutation in the active site of serine palmitoyltransferase causes catalytic promiscuity. *J. Biol. Chem.* **285,** 22846–22852
31. Penno, A., Reilly, M. M., Houlden, H., Laurá, M., Rentsch, K., Niederkofler, V., Stoeckli, E. T., Nicholson, G., Eichler, F., Brown, R. H., Jr., von Eckardstein, A., and Hornemann, T. (2010) Hereditary sensory neuropathy type 1 is caused by the accumulation of two neurotoxic sphingolipids. *J. Biol. Chem.* **285,** 11178–11187
32. De Luca, G., Calpona, P. R., Caponetti, A., Macaione, V., Di Benedetto, A., Cucinotta, D., and Di Giorgio, R. M. (2001) Preliminary report: amino acid profile in platelets of diabetic patients. *Metabolism* **50,** 739–741
33. Bertea, M., Rütti, M. F., Othman, A., Marti-Jaun, J., Hersberger, M., von Eckardstein, A., and Hornemann, T. (2010) Deoxysphingoid bases as plasma markers in diabetes mellitus. *Lipids Health Dis.* **9,** 84
34. Othman, A., Rütti, M. F., Ernst, D., Saely, C. H., Rein, P., Drexel, H., Porretta-Serapiglia, C., Lauria, G., Bianchi, R., von Eckardstein, A., and Hornemann, T. (2012) Plasma deoxysphingolipids: a novel class of biomarkers for the metabolic syndrome? *Diabetologia* **55,** 421–431
35. Othman, A., Saely, C. H., Muendlein, A., Vonbank, A., Drexel, H., von

Eckardstein, A., and Hornemann, T. (2015) Plasma 1-deoxysphingolipids are predictive biomarkers for type 2 diabetes mellitus. *BMJ Open Diabetes Res. Care* **3,** e000073
36. Scharff, R., and Wool, I. G. (1966) Effect of diabetes on the concentration of amino acids in plasma and heart muscle of rats. *Biochem. J.* **99,** 173–178
37. Mochida, T., Tanaka, T., Shiraki, Y., Tajiri, H., Matsumoto, S., Shimbo, K., Ando, T., Nakamura, K., Okamoto, M., and Endo, F. (2011) Time-dependent changes in the plasma amino acid concentration in diabetes mellitus. *Mol. Genet. Metab.* **103,** 406–409
38. McCampbell, A., Truong, D., Broom, D. C., Allchorne, A., Gable, K., Cutler, R. G., Mattson, M. P., Woolf, C. J., Frosch, M. P., Harmon, J. M., Dunn, T. M., and Brown, R. H., Jr. (2005) Mutant SPTLC1 dominantly inhibits serine palmitoyltransferase activity *in vivo* and confers an age-dependent neuropathy. *Hum. Mol. Genet.* **14,** 3507–3521
39. Eichler, F. S., Hornemann, T., McCampbell, A., Kuljis, D., Penno, A., Vardeh, D., Tamrazian, E., Garofalo, K., Lee, H. J., Kini, L., Selig, M., Frosch, M., Gable, K., von Eckardstein, A., Woolf, C. J., *et al.* (2009) Overexpression of the wild-type SPT1 subunit lowers desoxysphingolipid levels and rescues the phenotype of HSAN1. *J. Neurosci.* **29,** 14646–14651
40. Ehmsen, J. T., Ma, T. M., Sason, H., Rosenberg, D., Ogo, T., Furuya, S., Snyder, S. H., and Wolosker, H. (2013) D-Serine in glia and neurons derives from 3-phosphoglycerate dehydrogenase. *J. Neurosci.* **33,** 12464–12469
41. Hashemi, H. F., and Goodman, J. M. (2015) The life cycle of lipid droplets. *Curr. Opin. Cell Biol.* **33,** 119–124
42. Hapala, I., Marza, E., and Ferreira, T. (2011) Is fat so bad? Modulation of endoplasmic reticulum stress by lipid droplet formation. *Biol. Cell* **103,** 271–285
43. Hanada, K. (2003) Serine palmitoyltransferase, a key enzyme of sphingolipid metabolism. *Biochim. Biophys. Acta* **1632,** 16–30
44. Marshall, L. L., Stimpson, S. E., Hyland, R., Coorssen, J. R., and Myers, S. J. (2014) Increased lipid droplet accumulation associated with a peripheral sensory neuropathy. *J. Chem. Biol.* **7,** 67–76
45. Christofk, H. R., Vander Heiden, M. G., Harris, M. H., Ramanathan, A., Gerszten, R. E., Wei, R., Fleming, M. D., Schreiber, S. L., and Cantley, L. C. (2008) The M2 splice isoform of pyruvate kinase is important for cancer metabolism and tumour growth. *Nature* **452,** 230–233
46. Kung, C., Hixon, J., Choe, S., Marks, K., Gross, S., Murphy, E., DeLaBarre, B., Cianchetta, G., Sethumadhavan, S., Wang, X., Yan, S., Gao, Y., Fang, C., Wei, W., Jiang, F., *et al.* (2012) Small molecule activation of PKM2 in cancer cells induces serine auxotrophy. *Chem. Biol.* **19,** 1187–1198
47. Levy, M., and Futerman, A. H. (2010) Mammalian ceramide synthases. *IUBMB Life* **62,** 347–356
48. Michel, C., van Echten-Deckert, G., Rother, J., Sandhoff, K., Wang, E., and Merrill, A. H., Jr. (1997) Characterization of ceramide synthesis. A dihydroceramide desaturase introduces the 4,5-trans-double bond of sphingosine at the level of dihydroceramide. *J. Biol. Chem.* **272,** 22432–22437
49. Causeret, C., Geeraert, L., Van der Hoeven, G., Mannaerts, G. P., and Van Veldhoven, P. P. (2000) Further characterization of rat dihydroceramide desaturase: tissue distribution, subcellular localization, and substrate specificity. *Lipids* **35,** 1117–1125
50. Kamaura, M., Nishijima, K., Takahashi, M., Ando, T., Mizushima, S., and Tochikubo, O. (2010) Lifestyle modification in metabolic syndrome and associated changes in plasma amino acid profiles. *Circ. J.* **74,** 2434–2440